HIGH ENERGY NUCLEAR COLLISONS IN THE NA49 DETECTOR

H. Ströbele[10], H. Appelshäuser[7], J. Bächler[5], S.J. Bailey[16], L.S. Barnby[3], J. Bartke[6], R.A. Barton[3], H. Bialkowska[14], A. Billmeier[10], C.O. Blyth[3], R. Bock[7], C. Bormann[10], F.P. Brady[8], R. Brockmann[7], R. Brun[5], P. Bunčić[5,10], H.L. Caines[3], D. Cebra[8], G.E. Cooper[2], J.G. Cramer[16], P. Csato[4], J. Dunn[8], V. Eckardt[13], F. Eckhardt[12], M.I. Ferguson[5], H.G. Fischer[5], D. Flierl[10], Z. Fodor[4], P. Foka[10], P. Freund[13], V. Friese[12], M. Fuchs[10], F. Gabler[10], J. Gal[4], M. Gaździcki[10], E. Gladysz[6], J. Grebieszkow[15], J. Günther[10], J.W. Harris[17], S. Hegyi[4], T. Henkel[12], L.A. Hill[3], I. Huang[2,8], H. Hümmler[10], G. Igo[11], D. Irmscher[2,7], P. Jacobs[2], P.G. Jones[3], K. Kadija[18,13], V.I. Kolesnikov[9], M. Kowalski[6], B. Lasiuk[11,17], P. Lévai[4] A.I. Malakhov[9], S. Margetis[2], C. Markert[7], G.L. Melkumov[9], A. Mock[13], J. Molnár[4], J.M. Nelson[3], M. Oldenburg[10], G. Odyniec[2], G. Palla[4], A.D. Panagiotou[1], A. Petridis[1], A. Piper[12], R.J. Porter[2], A.M. Poskanzer[2], S. Poziombka[10], D.J. Prindle[16], F. Pühlhofer[12], W. Rauch[13], J.G. Reid[16], R. Renfordt[10], W. Retyk[15], H.G. Ritter[2], D. Röhrich[10], C. Roland[7], G. Roland[10], H. Rudolph[2,10], A. Rybicki[6], A. Sandoval[7], H. Sann[7], A.Yu. Semenov[9], E. Schäfer[13], D. Schmischke[10], N. Schmitz[13], S. Schönfelder[13], P. Seyboth[13], J. Seyerlein[13], F. Sikler[4], E. Skrzypczak[15], G.T.A. Squier[3], R. Stock[10], I. Szentpetery[4], J. Sziklai[4], P. Szymanski[10,14], M. Toy[2,11], T.A. Trainor[16], S. Trentalange[11], T. Ullrich[17], M. Vassiliou[1], G. Vesztergombi[4], D. Vranić[5,18], F. Wang[2], D.D. Weerasundara[16], S. Wenig[5], C. Whitten[11], T. Wienold[2], L. Wood[8], T.A. Yates[3], J. Zimanyi[4], X.-Z. Zhu[16], R. Zybert[3]

[1] *Department of Physics, University of Athens, Athens, Greece.* [2] *Lawrence Berkeley National Laboratory, University of California, Berkeley, USA.* [3] *Birmingham University, Birmingham, England.* [4] *KFKI Research Institute for Particle and Nuclear Physics, Budapest, Hungary.* [5] *CERN, Geneva, Switzerland.* [6] *Institute of Nuclear Physics, Cracow, Poland* [7] *Gesellschaft für Schwerionenforschung (GSI), Darmstadt, Germany.* [8] *University of California at Davis, Davis, USA.* [9] *Joint Institute for Nuclear Research, Dubna, Russia.* [10] *Fachbereich Physik der Universität, Frankfurt, Germany.* [11] *University of California at Los Angeles, Los Angeles, USA.* [12] *Fachbereich Physik der Universität, Marburg, Germany.* [13] *Max-Planck-Institut für Physik, Munich, Germany.* [14] *Institute for Nuclear Studies, Warsaw, Poland.* [15] *Institute for Experimental Physics, University of Warsaw, Warsaw, Poland.* [16] *Nuclear Physics Laboratory, University of Washington, Seattle, WA, USA.* [17] *Yale University, New Haven, CT, USA* [18] *Rudjer Boskovic Institute, Zagreb, Croatia.*

The energy density achieved in the early stage of high energy nucelar collisions is correlated with the rapidity loss of the participant nucleons. The produced π mesons seem to be insensitive to the variations of the corresponding energy loss. The K-mesons are enhanced with respect to the pions and have larger transverse momenta in heavy than in light collision systems. It turns out that the mean transverse momenta depend on the particle mass. This effect increases with system size suggesting a scenario in which a common transverse expansion velocity is superimposed on the normal chaotic motion. This picture is supported by results from 2-π correlation analysis, in which similar observations are made. The information from single partilce spectra and 2-π correlations lead to a freeze-out temperature around 120 MeV and a flow velocity of 0.6c.

1 Introduction

The ultimate goal of the CERN heavy ion program and similar studies foreseen at future collider facilities is the production and characterisation of an extended volume of equilibrated partonic matter, the quark gluon plasma (QGP)[1]. A phase transition to this state has been predicted by lattice QCD calculations (see[2] for recent reviews) for energy densities above 1–2 GeV/fm^3 and temperatures above a critical value T_c of about 180 to 200 MeV. In heavy ion collisions, if a QGP were indeed formed, it would be established in the early stage of the collision, after an initial pre-equilibrium state. Subsequently we expect a hadronisation of the partonic matter, followed by hadronic rescattering, chemical freeze-out and finally thermal freeze-out. Clearly, experimental information on the dynamics of the source evolution is required to reconstruct the initial conditions of the strongly interacting system and to verify whether or not this picture is realized. In this paper we present recent results from NA49 on participant protons, pions, and strange particles and study their production characteristics. The data from the heavy Pb+Pb system are compared to those from ^{32}S+ ^{32}S collisions in terms of baryon stopping, strange meson production and transverse momentum spectra.

2 Experimental Setup

The NA49 experiment is a large acceptance hadron spectrometer used for studies of proton+proton (p+p), proton+nucleus (p+A) and nucleus+nucleus (A+A) collisions at the CERN SPS. The experimental setup comprises four large volume Time Projection Chambers (TPCs) for charged particle tracking and identification by energy loss measurements, and four Time-of-Flight walls for additional particle identification (see also[3]). The acceptance covers about 80% of all charged particles for every event, leading to about 1200 detected particles in a single central Pb+Pb collision. For the analysis presented in this paper the 5% most central interactions were selected by a trigger on the energy deposited in the NA49 forward calorimeter. This corresponds to an impact parameter range of $b < 3.5$ fm.

3 Early Stage

Important information on the initial conditions in nuclear collisions can be obtained from a measurement of the distribution of net-baryons in the final state. The energy deposited by the incident nucleons in the reaction zone corresponds to a rapidity shift of these same nucleons from projectile and target rapidity towards midrapidity. Rapidity shifts of one unit near projectile rapidity translate into an energy loss (in the cms) of 5 GeV whereas the corresponding number near midrapidity is 1GeV only. This means that a comparison of different systems in terms of proton stopping should give more weight to protons abundances at large c.m. rapidities than to the details of the rapidity distribution near midrapidity. On the other hand thermalization and equilibration will affect preferentially the midrapidity nucleons. Proton rapidity distributions in

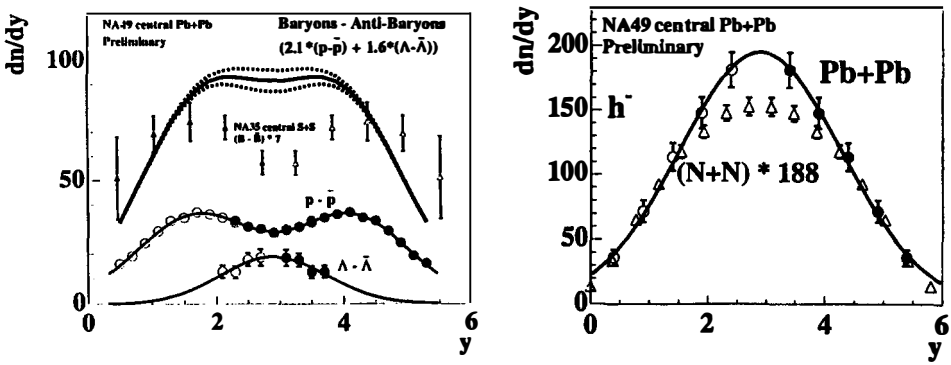

Figure 1: Rapidity distributions (left) for net-protons, net-Λ and net-baryons (solid line, see text) for Pb+Pb collisions; for comparison, the net-baryon distribution for central S+S (triangles) is also shown, scaled up by a factor of 7. Same (rigth) for negatively charged hadrons.

nucleon-nucleon interactions are known to exhibit a forward- backward peaked rapidity distribution with no yield at midrapidity. The corresponding distribution for nucleus-nucleus collisions are shown in Fig. 1, along with the distribution for net-baryons (solid line). The distribution for baryons minus anti-baryons was determined from the sum of $2.1 \times (p - \bar{p})$ and $1.6 \times (\Lambda - \bar{\Lambda})$, where the scale factors account for neutrons and higher mass hyperons, respectively.
In contrast to earlier measurements [3] the proton distribution in Fig. 1 was derived using the particle identification provided by energy loss measurement over a large acceptance, rather than measuring the net-charge distribution alone. Also, the correction for the contribution from decays of Λ and $\bar{\Lambda}$ was based on the distributions measured by NA49, rather than yields extracted from an event generator (VENUS 4.12).

Due to the decay-proton corrections the distributions of net-lambdas and net-protons are strongly correlated. In the net-baryon rapidity distribution this correlation however approximately cancels, which makes this a much better observable for systematic comparisons.
We observe a plateau in the net-baryon rapidity distribution, extending over two units of rapidity, with a rather sharp drop in the net-baryon rapidity density towards high and low rapidities. This can be compared to the properly scaled central S+S net-baryon distribution from NA35, which shows significantly higher yields near target and beam rapidity and the indication of a dip close to central rapidity. The additional energy lost by the incident nucleons in central collisions of heavy systems is not entirely spent to produce new particles. It also goes into higher transverse energy of the nucleons, as is demonstrated in Fig. 2. Here we show the slope factor

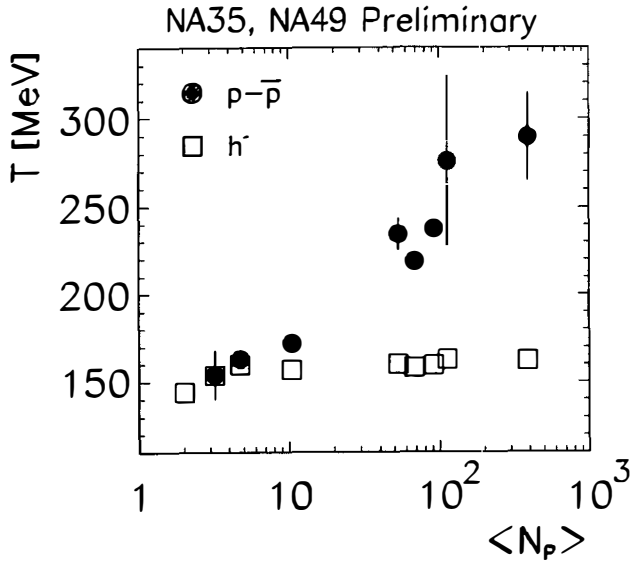

Figure 2: Inverse slope parameter T obtained from the invariant transverse momentum distributions of participant protons and negatively charged particles (for the latter T was obtained from the average transverse momentum) as function of the number of participant nucleons at SPS energy.

(T) determined from the transverse mass distribution of the participating nuleons determined near midrapidity. It is obvious that the slope factor shows a strong increase with system size which is represented by the number of participating nucleons. In summary the participating nucleons are sensitive to the system size both in their longitudinal and transverse motion.

In the following section we discuss the energy flow from the initial state nucleons to particles produced in the final state.

4 Produced Particles

Pions are the most abundantly produced particles. Their rapidity distribution is to a large degree independent of the size of the colliding objects as long as only symmetric systems are considered (see Fig. 1 right)[4,3]. Also, their mean transverse momentum changes by less than 10% when going from nucleon-nucleon to central Pb+Pb collisons (see Fig. 2). The pion production probability (per participating nucleon) increases only slightly (10-15%) from nucleon-nucleon to nuclear collisions [5]. In contrast to the results on the participant protons we find only little sensitivity of the shapes of the longitudinal and transverse momentum distributions of the pions on the system size.

The situation is quite different for the heavy K-mesons. Their production probability increases by almost a factor of two when comparing nucleon-nucleon with nuclear collisions. This is shown in Fig. 3, in which the K/π ratio is shown as a function of the number of participant

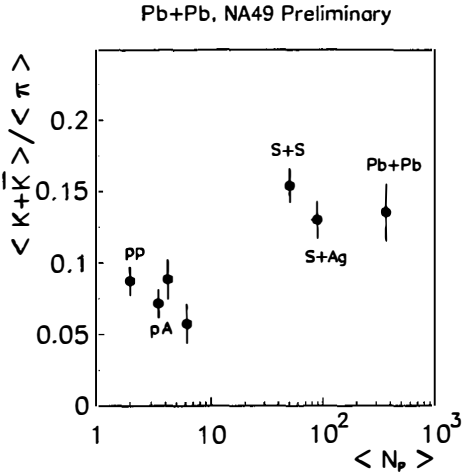

Figure 3: K/π ratio for different collision systems at SPS energy as function of the number of participant nucleons.

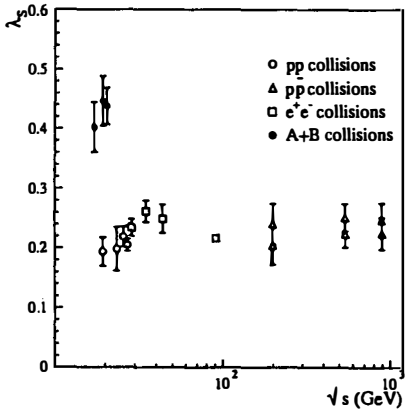

Figure 4: The strangeness suppression factor in high energy collisions is shown for various collision systems as function of $s^{1/2}$

nucleons. It is intriguing, however, to see that this strangeness enhancement (relativ to pions) occurs already for the light system ^{32}S+^{32}S and that no further increase for the very heavy system Pb+Pb is observed. Another interesting experimental finding is shown in in Fig. 4 in which the strangeness suppression factor[6] in A+A, nucleon+nucleon and e^++e^- collisions is shown as function of $\sqrt{s}$; the strangeness enhancement in A+A at $\sqrt{s}$=20 is much higher than in hadronic or leptonic interactions at much higher $\sqrt{s}$ (e.g.=1000 GeV). The data on K-distributions in logitudinal momentum space for the Pb+Pb are not yet accurate enough to make quantitative statements about any systematic variation with system size.

We turn now to the transverse momentum distributions of the produced particles. A summary of new results on single particle transverse momentum distributions for Pb+Pb collisions is shown in Fig. 5, where the inverse slope parameter T was obtained from a fit to the transverse mass spectrum using $\frac{1}{m_\perp}\frac{dn}{dm_\perp} = C\exp(-\frac{m_\perp}{T})$. One clearly observes an increase in the inverse slope parameter, for both mesons and baryons, with increasing particle mass. It is particularly interesting to note that protons and ϕ-mesons, which are similar in mass, also show very similar inverse slope parameters of around 290 MeV. Another intriguing result is the inverse slope of the deuteron spectrum of $\approx$ 380 MeV.
Clearly an inverse slope of this magnitude, more than two times higher than the limiting 'Hagedorn' temperature, cannot be interpreted as a temperature of a hadronic system. The simplest extension of a thermal model is the introduction of a transverse velocity field which is common

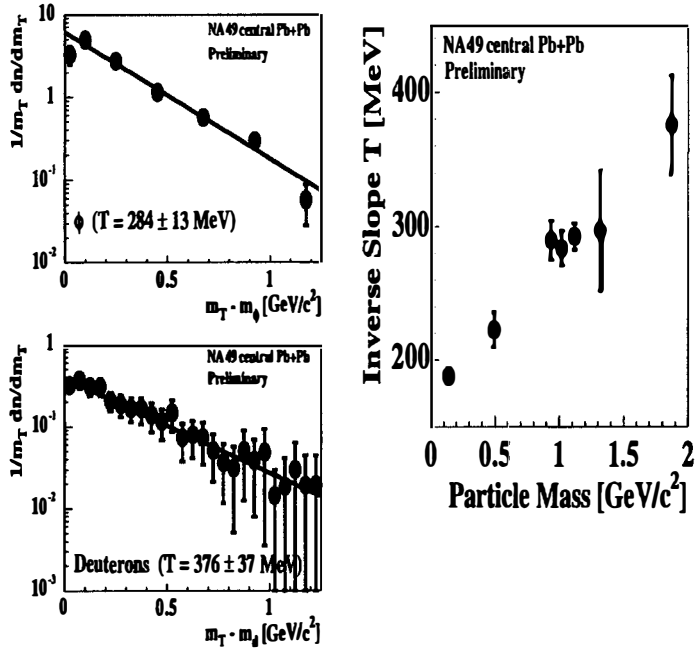

Figure 5: Inverse slope parameters for various hadron species in central Pb+Pb collisions.

to all particles. This naturally leads to the observed dependence of inverse slopes on the particle mass[7]. It has been shown in several publications that, with the choice of an appropriate velocity profile, such an extended model can indeed describe the inverse slope systematics with just two parameters, a common thermal freeze-out temperature T_f and a flow velocity parameter $\beta_\perp$ that characterizes the strength of the flow velocity field and is common to all particle species [8,9,10,11]. It has also been shown that the minima in the goodness-of-fit parameter as a function of the parameters T_f and $\beta_\perp$ are rather shallow, with a strong correlation between the parameters, leading to a large uncertainty in particular in the determination of $\beta_\perp$ [8]. To resolve this ambiguity independent information on the flow velocity is required. Such information can be obtained in a quantitative fashion from two-particle Bose-Einstein correlations.

The theoretical framework for this measurement has been considerably refined recently [12]. Using the dependence of the two-particle correlation function in relative momentum on the average pair momentum, which reflects the correlation between position and momentum of particles in an expanding source, it is now possible to extract dynamical parameters like expansion velocities and lifetime from the correlation measurement.
It has been demonstrated in [9] that a convenient way to parametrize the correlation function is given by the Yano-Koonin-Podgoretsky formalism, where the correlation function is written as

$$C_2(Q_\perp, Q_\parallel, Q_0, y_{\pi\pi}, k_\perp) = 1 + \lambda exp\,[-Q_\perp^2 R_\perp^2 - \gamma_{YK}^2 (Q_\parallel - \beta_{YK} Q_0)^2 R_\parallel^2 - \gamma_{YK}^2 (Q_0 - \beta_{YK} Q_\parallel)^2 R_0^2].$$

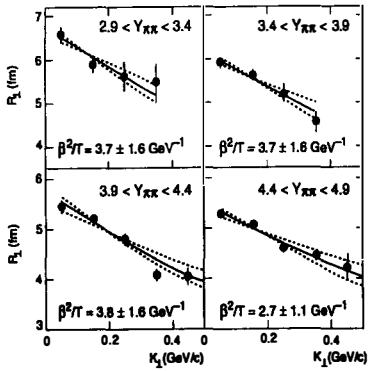

Figure 6: Dependence of the transverse correlation length $R_\perp$ on the average transverse momentum $k_\perp$ of the pion pair. The fit to the data determins the ratio of the flow velocity parameter $\beta_\perp$ and the thermal freeze-out temperature T_f.

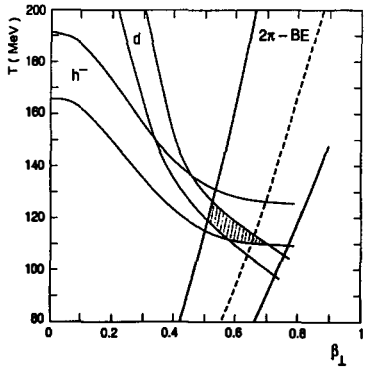

Figure 7: Thermal freeze-out temperature T_f versus transverse flow velocity parameter $\beta_\perp$ obtained from central Pb+Pb collisions. The curves show constraints from fits to single-particle transverse mass spectra and two-particle correlation analysis.

Here the colliding system is described as a row of local source elements along the longitudinal axis, where each element is characterized by its space-time extent ($R_\parallel(k_\perp, y_{\pi\pi})$, $R_\perp(k_\perp, y_{\pi\pi})$, $R_0(k_\perp, y_{\pi\pi})$) and longitudinal velocity $\beta_{YK}(k_\perp, y_{\pi\pi})$ and $k_\perp$ and $y_{\pi\pi}$ are the average transverse momentum and rapidity of the pion pair. The parametrization is then fitted to the measured three dimensional correlation function in bins of rapidity and transverse momentum. As we are dealing with central events, we can savely average over the azimuthal angle. The experimental correlation function was corrected for the final-state Coulomb interaction using a scheme based on the measured correlation function for unlike-sign pions[14,15]. Further experimental details are described in [14].

Fig. 6 shows that for the transverse radius parameter a clear dependence on transverse momentum is observed. This provides information on the strength of the transverse velocity field, as was shown in [9]. By fitting the source function from [9] to the correlation data, a value of $\beta_\perp^2/T_f = (3.7 \pm 1.5)$ GeV^{-1} is determined. Again, the values for the expansion velocity and the thermal freeze-out temperature are correlated, as was the case for the fit to the single particle spectra. However, for the two-particle correlations, as is shown in Fig. 7 [13], the valley for the χ^2-minimum runs almost perpendicular to that for the single particle spectra. By combining the information from single- and two-particle spectra one can therefore tightly constrain $\beta_\perp$ and T_f at the same time. The allowed region in Fig. 7 suggests that thermal freeze-out occurs at $T_f \approx 120$ MeV and $\beta_\perp \approx 0.55$. So far the influence of resonance decays has not been taken into account consistently in this analysis.

5 Summary and Conclusions

New results on particle abundances in Pb+Pb collisions are consistent with the strangeness enhancement observed in earlier measurements of central collisions between lighter projectiles at the SPS. The inverse slopes of transverse mass distributions for different hadrons in central

Pb+Pb collisions exhibit a significant dependence on the hadron mass. This finding suggests a collective transverse velocity field, a hypothesis which is supported by the dependence of the transverse radius parameter on the pair transverse momentum observed in an analysis of two particle Bose-Einstein correlations.
A fit with a source function inspired by a hydrodynamical picture of the collision yields a rather low thermal freeze-out temperature of $T_f \approx 120$ MeV and an expansion velocity of $\beta_\perp \approx 0.55$.

Acknowledgements: This work was supported by the Director, Office of Energy Research, Division of Nuclear Physics of the Office of High Energy and Nuclear Physics of the US Department of Energy under Contract DE-AC03-76SF000 98, the US National Science Foundation, the Bundesministerium fur Bildung und Forschung, Germany, the Alexander von Humboldt Foundation, the UK Engineering and Physical Sciences Research Council, the Polish State Committee for Scientific Research (2 P03B 01912), the Hungarian Scientific Research Foundation under contracts T1492 and T7330, the EC Marie Curie Foundation, and the Polish-German Foundation.

1. J. C. Collins and M. J. Perry, Phys. Rev. Lett. **34** (1975) 1353,
   E. V. Shuryak, Phys. Rep. **C61** (1980) 71 and **C115** (1984) 151
2. E. Laermann, Nucl. Phys. **A610** (1996) 1,
   E. Laermann, Proceedings of the Hirschegg Workshop on QCD Phase transitions, 1997
3. P. Jones et al. (NA49 Collaboration), Nucl. Phys. **A610** (1996) 188
4. p+p,p+n at 200 GeV/N: Y. Eisenberg et al., Nucl. Phys. **B154** (1979) 239
   C. De Marzo et al., Phys. Rev. **D26** (1982) 1019
5. M. Gaździcki, D. Röhrich, Z. Phys. **C65** (1995) 215
6. F. Becattini, M. Gazdzicki and J. Sollfrank; IKF-HENPG/4-97, subm. to Europhys. Journal C 1998
7. J. Sollfrank et al., Z. Phys. **C52** (1991) 593, E. Schnedermann et al., Phys. Rev. **C48** (1993) 2462
8. B. Kämpfer, preprint FZR-149, hep-ph/9612336 preprint
9. U. Heinz, Nucl. Phys. **A610** (1996) 264
10. U. Wiedemann et al., nucl-th/9611031 preprint
11. J. Alam, J. Cleymans, K. Redlich, H. Satz, nucl-th/970742 preprint
12. S. Pratt, Phys. Rev. **D33** (1986) 1314, A. N. Maklin and Y. M. Sinyukov, Z. Phys. **C39** (1988) 69; G. Bertsch, Nucl. Phys. **A498** (1989) 173 S. Chapman, J. R. Nix and U. Heinz, Phys. Rev. **C52** (1995) 2694, S. Pratt, Phys. Rev. **D33** (1986) 1314
13. H. Appelshäuser et al., IKF-HENPG-6-97 (hep-ex/9711024) and to be published in Eur. Phys. J. A 1998
14. H. Appelshäuser, PhD thesis Frankfurt 1997, S. Schönfelder, PhD thesis, MPI Munich 1997, MPI-PhE/97-09
15. T. Alber et al., Z. Phys. **C73** (1997) 443